



Laval (Greater Montreal)

June 12 - 15, 2019

EVALUATION OF STEEL FIBRE REINFORCED CONCRETE BEAMS UNDER ULTIMATE AND SERVICEABILITY LIMIT STATES

Helmi Alguhi¹ and Douglas Tomlinson²

^{1,2} University of Alberta, Canada

¹ alguhi@ualberta.ca

Abstract: Steel-fibre reinforced concrete (SFRC) is used in many construction applications such as shotcrete tunnel walls and slabs on grade. Compared to non-fibre reinforced concrete, SFRC has superior post-cracking performance that leads to elements with narrower crack widths. Narrower cracks enhance the service performance of beams and improve aggregate interlock, which increases the shear capacity of SFRC members relative to non-fibre reinforced concrete. However, the benefits of using SFRC are not incorporated into the design standard for concrete buildings (A23.3-14), particularly for crack control and shear resistance. The steel fibre contribution is modelled by changing the concrete's tension stress-strain response based on an inverse analysis of experimental test data of 30 and 50 MPa beams with fibre dosages between 0.5 and 1.0 %. Three full scale (2800 x 300 x 150 mm) beams were analyzed in this study with eight variations per beam. In total, 24 models with varying concrete strength, fibre reinforcement ratio, and shear reinforcement were investigated. The results show that SFRC is most effective at improving the strength of members without stirrups. SFRC has smaller crack widths and enhanced aggregate interlock compared to non-fibre reinforced concrete. The effectiveness of SFRC increased with fibre dosage, particularly for fibres with hooked ends. The failure mode can be changed from diagonal shear failure to flexural failure in members with no or limited shear reinforcement.

1 INTRODUCTION

Concrete has a low tensile strength compared to its compressive strength. It also has a low deformation capacity, resulting in a brittle material. This is a particular disadvantage when the material is used for members with lower flexural stiffness such as lightly or glass fibre reinforced polymer (GFRP) reinforced beams that develop wide cracks and low ultimate shear strength relative to than members with high flexural stiffness.

It is generally accepted that ductility of concrete mixtures can be improved by adding adding steel fibres into the concrete matrix. This results in Steel Fibre Reinforced Concrete (SFRC). Several techniques have been proposed to determine the tensile stress-strain (σ - ϵ) relationship of Steel Fibre Reinforced Concrete (SFRC). Lim et al. developed a tensile σ - ϵ relationship using laws of mixture and results from steel fibre pullout tests (Lim et al. 1987). A similar method was proposed by Lok and Pei with some modifications, (Lok and Pei 1998). RILEM TC 162-TDF (Vandewalle 2000) and Barros et al. (Barros and Figueiras 2001) proposed a tensile σ - ϵ relationship that uses results from a deformation-controlled beam-bending test to determine the peak and post-cracking stresses. The work presented in this study will focus on an inverse analysis which is a more general approach and so is becoming more attractive and gaining the attention of researchers in the past few years e.g., (Elsaigh et al. 2004; Hemmy 2002; Kohoutkova et al. 2004; Labib 2008; Tlemat et al. 2006).

VecTor2[®] is a 2D finite element software developed at the University of Toronto that is based on Modified Compression Field Theory (MCFT) (Wong et al. 2013). MCFT analysis, demonstrates that SFRC has smaller crack widths and so enhanced aggregate interlock compared to non-fibre reinforced concrete that leads to improved shear strength. Previous research has been conducted on the shear performance of SFRC beams (Abbas et al. 2014; Cucchiara et al. 2004; Ding et al. 2011; Dinh 2009; Lim and Oh 1999; Minelli et al. 2014). However, there are limited studies on of the effect of SFRC on crack width and its effect on shear performance. Therefore the research presented in this paper considers the crack width under service loads.

2 DESCRIPTION OF EXPERIMENTAL PROGRAM

The experimental program was conducted at King Saud University to study the effect of fibre content on the flexural behaviour of SFRC for on-grade slab applications. The load-deflection results of SFRC prisms from that program are used to verify the upcoming inverse analysis. Beam specimens measuring 150 x 150 x 600 mm under four-point loading were tested in displacement control at a rate of 0.2 mm/min. The two point loads were applied symmetrically 150 mm apart. The prism supports were bolted to the machine body and set 450 mm apart. Mid-span deflection was measured by using the average of two LVDTs located at mid-span on both sides of the prism. Two concrete strengths were considered (30 MPa and 50 MPa) and three different fibre reinforcement percentages were considered (0.5%, 0.76%, and 10% by volume), making for six overall mixtures.

3 NUMERICAL ANALYSIS

The Finite Element Analysis (FEA) program VecTor2[®] (version 4.2) was used (Wong 2013) for numerical analysis in this investigation. The FEA was divided into two phases: in Phase 1, where the constitutive model of SFRC was developed, and Phase 2 material model was used in a full scale model conduct a parametric study that considered fibre volume, concrete strength, and shear reinforcement. The two phases are summarized in Figure 1.

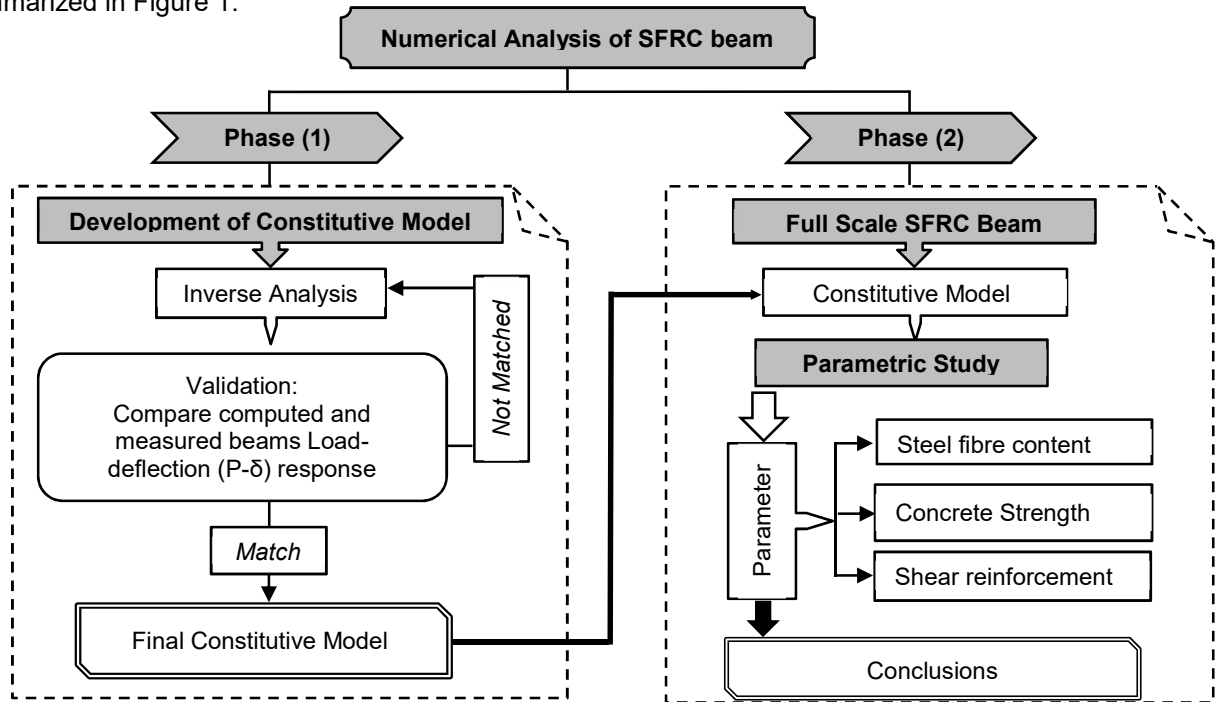


Figure 1: Numerical analysis of SFRC beam flow chart

3.1 Phase 1: Constitutive Model

3.1.1 Finite element model of prism tests

The prisms were divided into 144 hybrid rectangular elements with a 25 x 25 mm mesh size as shown in Figure 2. The same mesh dimensions were used and recommended for similar analyses conducted by other researchers e.g., (Blazejowski 2012; Labib 2008; Thomas and Ramaswamy 2007). Displacement control was used in this analysis and the boundary conditions of the model replicated those in the experimental setup.

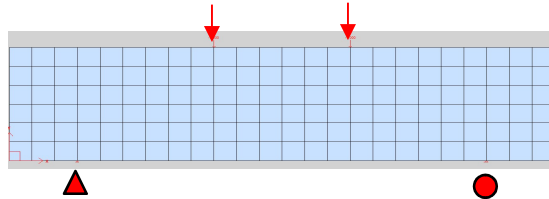


Figure 2: Mesh, loading and boundary condition

3.1.2 Inverse analysis

In an inverse analysis, an iterative procedure is used to derive the tensile behaviour of SFRC for each of the six mixtures. The tensile behaviour of SFRC is assumed to follow a tri-linear response (Figure 3), whereas point A peak stress (σ_1) is corresponding to crack load and B and C are matching to the residual stress σ_2 and σ_3 .

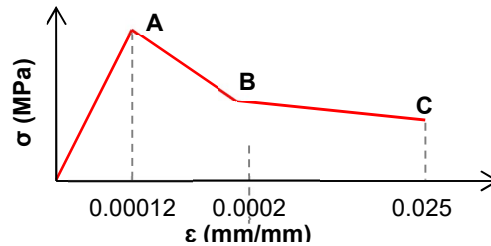


Figure 3: General form of the tri-linear stress-strain relationship for SFRC

The development of the tensile σ - ϵ relationship for a specific SFRC material (concrete strength, fibre type), Figure 4 includes the following four steps:

1. Obtain the load-deflection (P - δ) relationship from a four-point bending prism test for a particular SFRC mix design under consideration using previously established procedures (Aldossari 2014).
2. Choose a tri-linear tensile model (see Figure 3) to serve as the constitutive model.
3. Simulate the prism test using FEA using the constitutive model.
4. Use the results of Step 3 to adjust the tensile σ - ϵ relationship parameters in Step 2 (A,B, and C in Figure 3). Iterate until the experimental and numerically-determined load-deflection behaviour reach a reasonable match.

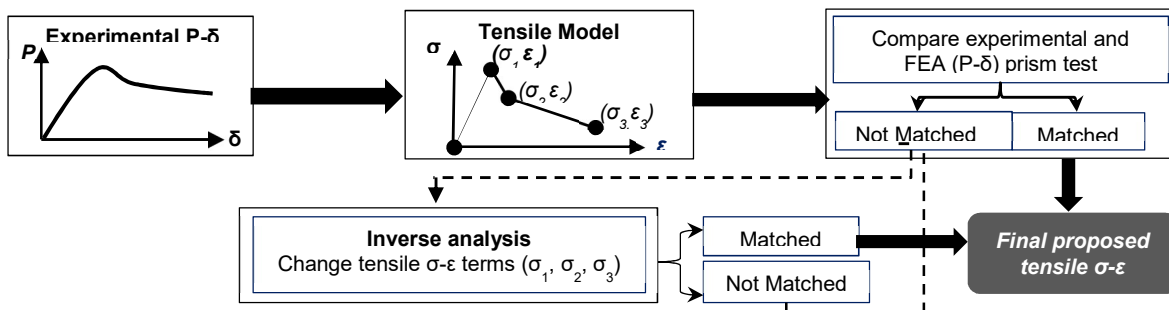


Figure 4: Inverse analysis process flow chart

3.2 Phase 2: Full-Scale Model

Three full-scale beam designs with two concrete strengths and three shear reinforcement ratios were considered: SFB-C (control beam without stirrups), SFB-5S (beam with 10M stirrups @ 250mm), and SFB-11S (beam with 10M stirrups @ 100mm). The full-scale beam dimensions are 2800 x 300 x 150 mm, the longitudinal reinforcement ratio is 1.33% in all cases, yield strength of steel is 475 MPa, and the stirrups are located in the shear zone at distance 100 mm from the point load to end of the beam as shown in Figure 5. Hybrid rectangular elements were selected to model the concrete. The concrete's tensile stress-strain response developed in Phase 1 adopted in the Phase 2 analysis. The beam was divided into 1456 elements with mesh size 25 x 25 mm (the same mesh dimensions were used in Phase 1). Truss elements were used to model longitudinal reinforcement; stirrups were modeled using smeared reinforcement properties.

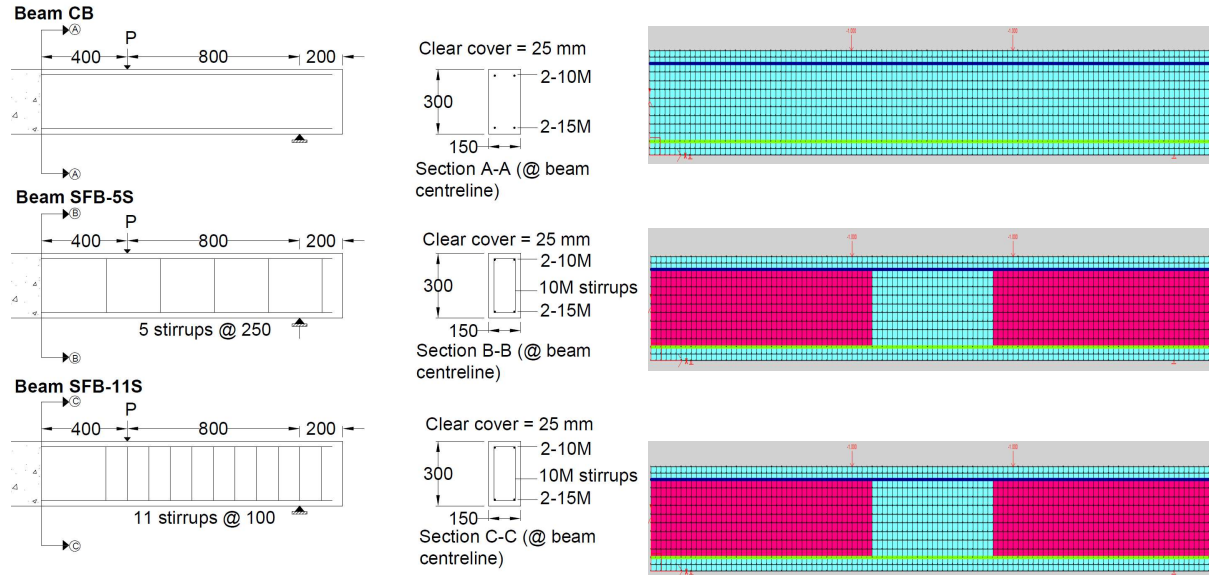


Figure 5: Proposed and modeled SFRC full scale beams

Parametric studies were conducted on the full-scale model to investigate the effect of concrete strength (30 and 50 MPa), fibre content (0%, 0.5%, 0.76%, and 1.0%), and shear reinforcement spacing on the beam response. Based on the FEA information, a deeper understanding of the performance of beams can be obtained for ultimate limit state in terms of shear strength, stiffness, and ductility and serviceability limit state in terms of crack width

4 RESULTS AND DISCUSSION

The parameters of the initial tensile σ - ϵ relationship, $\sigma_1, \sigma_2, \sigma_3, \epsilon_1, \epsilon_2,$ and ϵ_3 (see Figure 4) were adjusted in the model until the calculated and measured load-deflection (P - δ) behaviours matched. The experience gained from these iterations indicates that $\sigma_1, \sigma_2,$ and σ_3 are interrelated. In other words, their influence is not confined to a single part of the P - δ response. Changing σ_1 has considerable influence on the cracking load but little effect on the post-cracking plateau of the P - δ response. σ_2 and σ_3 remarkably affect the post-cracking relationship with minimal influence on the cracking load. The pre-cracking part of the P - δ response is influenced by the concrete's elastic modulus as discussed earlier. Keeping in mind the narrow range of strain values, the change in $\epsilon_1, \epsilon_2,$ and ϵ_3 were found to have an insignificant influence on the P - δ behaviour. Therefore, these strain values were kept unchanged at 0.00012, 0.002, and 0.025 during iterations (Figure 3).

After several iterations, $\sigma_1, \sigma_2,$ and $\sigma_3,$ the calculated P - δ behaviour in the prism test from the FEA reasonably matched the experimental results (Figure 6). The cracking loads, and the post-cracking P - δ response fit appropriately. The proposed tensile σ - ϵ relationship parameters for each volume fraction and concrete strength are given in Table 1.

Table 1: Proposed tensile stress-strain points for each concrete mixture

Concrete Strength, f'_c (MPa)	Fibre Volume Fraction, V_F , (%)	$A(\sigma_1)$ (MPa), $\epsilon = 0.00012$	$B(\sigma_2)$ (MPa), $\epsilon = 0.0002$	$C(\sigma_3)$ (MPa), $\epsilon = 0.025$
30	0.5	1.8	1.5	1.0
	0.76	2.2	2.0	2.0
	1.0	2.6	2.4	2.4
50	0.5	3	2.8	2.0
	0.76	3.8	3.4	2.8
	1.0	4.2	4.0	2.6

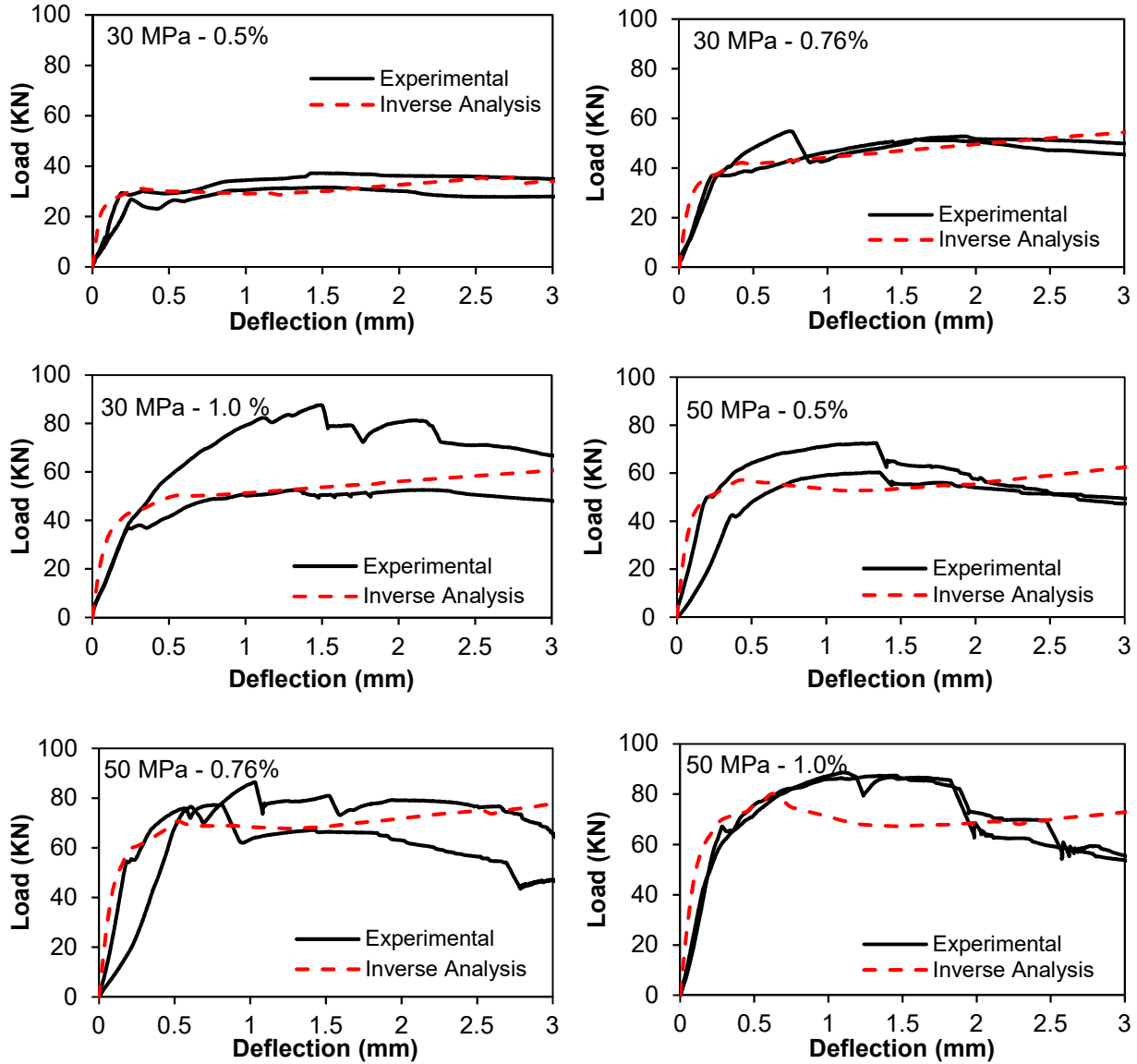


Figure 6: Computed and modeled load deflection responses for the six different mixtures

Figure 7 shows the load-deflection response of beams with different the concrete compressive strengths, steel fibre contents and stirrup spacings. The ultimate strength increased significantly and at pre-yielding load stage the section gains some stiffness due to the increased reinforcement ratio added by the steel fibres. The post-cracking response improved as well in terms of ductility. For example, adding 0.5% V_f to

30 MPa-CB increased the peak load by 48% from 79 kN to 117 kN and for 50 MPa-CB the the peak load goes up by 50% from 90 kN to 135 kN. In addition, the ductility of 0.5% V_f 30 MPa-CB increased 7 times compared to beams without steel fibres. Adding stirrups increases both ultimate shear strength and ductility.

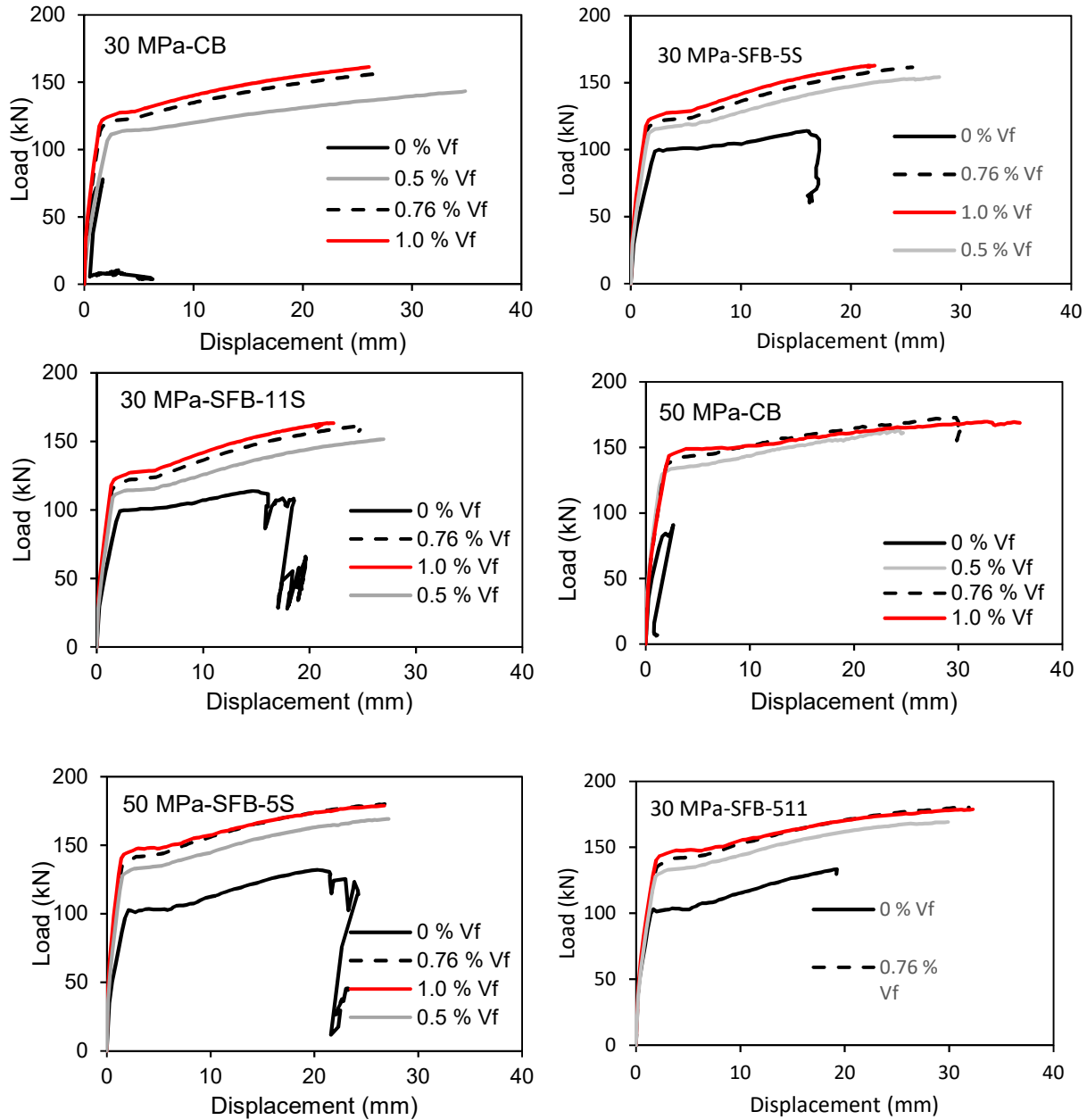


Figure 7: Load deflection responses of full-scale beam models

Flexural crack widths were extracted at a serviceability load equal to 65 kN for each beams. This load was determined based on dividing the yield load of the beam most representative of a typical beam, 30 MPa-SFB-11S-0.0%, by 1.5 (the load factor for live load in the National Building Code of Canada). Back calculations of factored loads were used to estimate service loads as these beams were not deflection-controlled (i.e. the typical deflection limit for beams, $L/360$, is 6.7 mm, higher than the yield deflection of all beams). The crack width reducing significantly by increasing the steel fibre content for each type of beam.

The higher the concrete strength the lower the flexural crack width because of the bond between the steel fibre content and concrete matrix goes up by increasing the compression strength as shown in Figure 8.

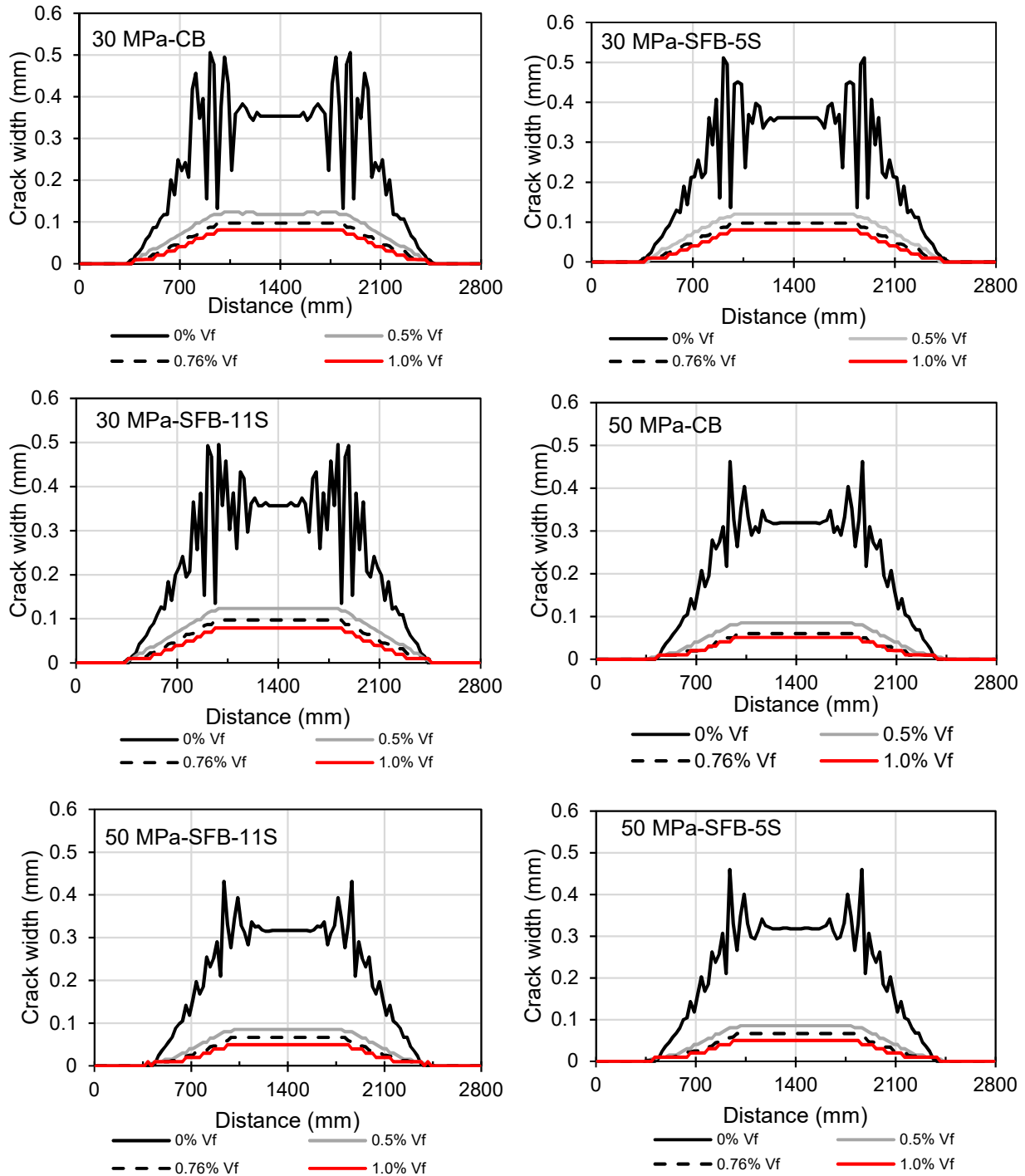


Figure 8: Crack widths along each beam under a service load of 65 kN.

Figure 9 compares the maximum flexural crack width extracted at the extreme tension fibre of the 30 MPa and 50 MPa beams. For example, adding 0.5% V_f to 30 MPa-CB leads to decrease the maximum crack width by 80% from 0.52 mm to 0.12 mm and for 50 MPa-CB the crack width reduced by 82% from 0.46 mm

to 0.08mm. The shear reinforcement has a negligible effect on the crack width at service loads at the extreme tension fibre.

The failure mode changed in beams without stirrups when steel fibres were added. The failure mode shifted from diagonal tension shear failure (brittle failure) to flexural tension (ductile failure) by adding steel fibre as shown in Figure 10. Table 2 shows the results summary of all beams.

Table 2: Model results summary

Beam	Deflection at service*, mm	Maximum Crack width at Service, mm	Yield Load, kN	Peak Load, kN	Deflection at Peak, mm	Ductility Index	Failure Mode**
30-CB-0	1.20	0.505	65	78	2.26	1.87	D.T.S
30-CB-0.5	1.01	0.124	105	143	33.56	16.73	F.T
30-CB-0.76	0.85	0.097	116	156	31.92	16.97	F.T
30-CB-1.0	0.76	0.081	121	161	31.73	14.36	F.T
30-SFB-5S-0.0	1.15	0.500	100	114	15.96	4.92	F.T
30-SFB-5S-0.5	0.70	0.122	111	150	14.69	9.12	F.T
30-SFB-5S-0.76	0.59	0.097	117	160	25.57	15.59	F.T
30-SFB-5S-1.0	0.50	0.080	123	163	22.14	12.10	F.T
30-SFB-11S-0.0	1.10	0.495	100	114	19.66	5.27	F.T
30-SFB-11S-0.5	0.70	0.121	112	152	26.95	13.82	F.T
30-SFB-11S-0.76	0.58	0.097	118	160	25.04	13.98	F.T
30-SFB-11S-1.0	0.50	0.079	125	163	22.26	9.23	F.T
50-CB-0	1.00	0.462	86	91	2.6	1.10	D.T.S
50-CB-0.5	0.43	0.085	129	163	23.68	15.80	F.T
50-CB-0.76	0.51	0.060	137	173	29.80	14.90	F.T
50-CB-1.0	0.50	0.051	143	170	32.78	14.90	F.T
50-SFB-5S-0.0	0.89	0.459	102	132	20.34	10.01	F.T
50-SFB-5S-0.5	0.43	0.085	127	169	27.14	18.21	F.T
50-SFB-5S-0.76	0.33	0.066	130	180	26.76	19.82	F.T
50-SFB-5S-1.0	0.27	0.050	144	179	26.72	15.72	F.T
50-SFB-11S-0.0	0.64	0.431	102	133	19.25	8.02	F.T
50-SFB-11S-0.5	0.60	0.085	128	169	29.90	16.00	F.T
50-SFB-11S-0.76	0.27	0.066	140	179	26.61	19.00	F.T
50-SFB-11S-1.0	0.45	0.049	145	179	30.60	17.52	F.T

* Service load is defined as 65 kN,** D.T.S is diagonal tension shear failure and F.T is flexural tension failure.

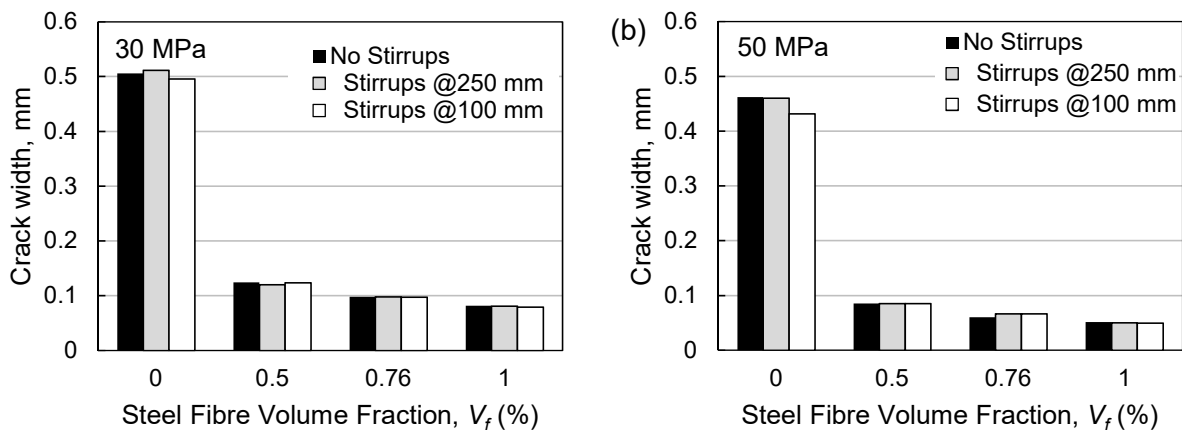


Figure9: Crack width comparison for different beam cases for (a) 30 MPa concrete strength, (b) 50 MPa concrete strength

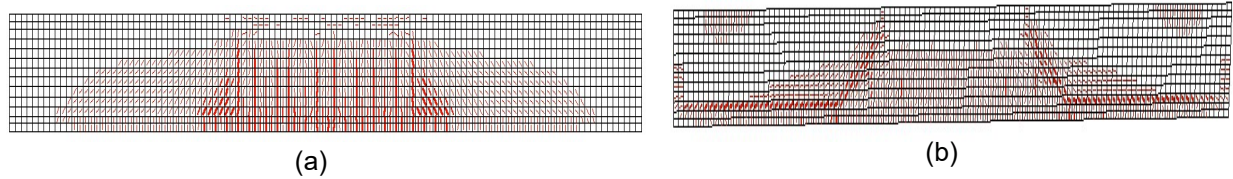


Figure 10: Failure mode at peak load for beams with 30 MPa concrete without stirrups (a) $V_f = 0.5\%$, (b) $V_f = 0.0\%$.

5 CONCLUSIONS AND RECOMMENDATIONS

A SFRC constitutive model was generated using inverse analysis for two concrete strengths, (30 and 50 MPa) and three steel fibre contents (0.5, 0.75 and 1.0 %). The constitutive model was used to model full-scale beams with different shear reinforcement configurations to study the effect of steel fibre content, concrete strength and stirrups on the beam's strength, ductility, deflection, and crack width. Based on the results presented in this paper, the following conclusions can be drawn:

1. The inverse analysis can be successfully implemented in VecTor2[®] to appropriately determine the tensile σ - ϵ relationship of SFRC beams.
2. The developed tensile σ - ϵ relationship is element-size dependent. For FEA analysis incorporating SFRC beams, the element size can be decided upon beforehand and the tensile σ - ϵ relationship can be generated accordingly.
3. Beam strength and ductility significantly increased with an increase in the steel fibre percentage for typical simply supported beams with 30 MPa and 50 MPa.
4. The failure mode changed from shear diagonal failure to flexural failure and crack width decreased significantly by adding steel fibres. Additionally, the higher the concrete strength the lower the crack width. In addition, the stirrups did not influence on the crack width in service loading and the stirrups can be partially replaced by steel fibres.

Based on the results, there is promise in using different chopped fibre with low modulus of elasticity materials such as GFRP to improve their shear resistance and crack width. These results should then be used to give predictions of experimental full scale FRP beams that are planned to evaluate the shear performance of reinforced beams with chopped fibres.

6 REFERENCES

- Abbas, A. A., Syed Mohsin, S. M., Cotsovos, D. M., and Ruiz-Teran, A. M. 2014. Shear Behaviour of Steel-Fibre-Reinforced Concrete Simply Supported Beams. *Proceedings of the Institution of Civil Engineers-Structures and Buildings*, **167**(9), 544-558.
- Aldossari, K.M. 2014. Behavior of High Strength Steel Fibers Reinforced Concrete Ground Slabs. Master, King Saud University, Saudi Arabia.
- Barros, J. A., and Figueiras, J. A. 2001. Model For The Analysis of Steel Fibre Reinforced Concrete Slabs on Grade. *Computers & Structures*, **79**(1), 97-106.
- Blazejowski, M. 2012. Flexural Behaviour Of Steel Fibre Reinforced Concrete Tunnel Linings.
- Cucchiara, C., La Mendola, L., and Papia, M. 2004. Effectiveness Of Stirrups And Steel Fibres As Shear Reinforcement. *Cement and concrete composites*, **26**(7), 777-786.
- Ding, Y., You, Z., and Jalali, S. 2011. The Composite Effect of Steel Fibres And Stirrups on The Shear Behaviour of Beams Using Self-Consolidating Concrete." *Engineering structures*, **33**(1), 107-117.
- Dinh, H. H. (2009). "Shear Behavior of Steel Fiber Reinforced Concrete Beams without Stirrup Reinforcement."

- Elsaigh, W., Robberts, J., and Kearsley, E. 2004. Modelling Non-Linear Behaviour of Steel Fibre Reinforced Concrete." *6th International RILEM Symposium on Fibre Reinforced Concretes*, 837-846.
- Hemmy, O. 2002. Recommendations for finite element analysis of FRC—report of subtask 3.5. *Brite-Euram project BRPR-CT98-0813: Test and Design Methods for Steel Fibre Reinforced Concrete, Project funded by the European Community under the Industrial and Materials Technologies Programme (Brite-Euram II)*.
- Kohoutkova, A., Kristek, V., and Broukalova, I. 2004. Material Model of FRC-Inverse Analysis. *Proc., Fibre-reinforced Concretes: Proceedings of the Sixth International RILEM Symposium*, RILEM Publications, 857-864.
- Labib, W. A. 2008. An experimental study and finite analysis of punching Shear Failure In Steel Fibre-Reinforced Concrete Ground-Suspended Floor Slabs. Liverpool John Moores University.
- Lim, D., and Oh, B. 1999. Experimental And Theoretical Investigation on The Shear of Steel Fibre Reinforced Concrete Beams." *Engineering structures*, **21**(10), 937-944.
- Lim, T., Paramasivam, P., and Lee, S. 1987. "Analytical Model for Tensile Behavior of Steel-Fiber Concrete." *ACI Materials Journal*, **84**(4).
- Lok, T.-S., and Pei, J.-S. 1998. Flexural Behavior of Steel Fiber Reinforced Concrete. *Journal of Materials in Civil engineering*, **10**(2), 86-97.
- Minelli, F., Conforti, A., Cuenca, E., and Plizzari, G. 2014. Are Steel Fibres Able to Mitigate or Eliminate Size Effect in Shear?" *Materials and structures*, **47**(3), 459-473.
- Thomas, J., and Ramaswamy, A. 2007. Mechanical Properties of Steel Fiber-Reinforced Concrete. *Journal of materials in civil engineering*, **19**(5), 385-392.
- Tlemat, H., Pilakoutas, K., and Neocleous, K. 2006. Modelling of SFRC Using Inverse Finite Element Analysis. *Materials and Structures*, **39**(2), 221-233.
- Vandewalle, L. (2000). Recommendations of RILEM TC 162-TDF: Test and design methods for steel fibre reinforced concrete." *Materials and Structures/Materiaux et Constructions*, 33(225), 3-5
- Wong, P., Vecchio, F., and Trommels, H. 2013. Vector2 & Formworks User's Manual Second Edition. Toronto, Canada.